



#### **OPEN ACCESS**

EDITED BY Alastair Stacey, RMIT University, Australia

Amit Finkler. Weizmann Institute of Science, Israel Connor Roncajoli. Army Research Laboratory, United States Santiago Corujeira Gallo, Quantum Brilliance, Germany

\*CORRESPONDENCE Jonas Nils Becker. ⊠ becke183@msu.edu Shannon Singer Nicley, ⊠ nicleysh@msu.edu

<sup>†</sup>These authors have contributed equally to this work and share last authorship

RECEIVED 16 July 2025 ACCEPTED 25 August 2025 PUBLISHED 23 September 2025

Klink K, Kirkpatrick AR, Tadokoro Y, Becker JN and Nicley SS (2025) Fabrication of oriented NV center arrays in diamond via femtosecond laser writing and reorientation.

Front. Quantum Sci. Technol. 4:1667545. doi: 10.3389/frqst.2025.1667545

© 2025 Klink, Kirkpatrick, Tadokoro, Becker and Nicley. This is an open-access article distributed under the terms of the Creative Commons Attribution License (CC BY). The use, distribution or reproduction in other forums is permitted, provided the original author(s) and the copyright owner(s) are credited and that the original publication in this journal is cited, in accordance with accepted academic practice. No use, distribution or reproduction is permitted which does not comply with these

# Fabrication of oriented NV center arrays in diamond via femtosecond laser writing and reorientation

Kai Klink<sup>1,2</sup>, Andrew Raj Kirkpatrick<sup>1,2</sup>, Yukihiro Tadokoro<sup>3</sup>, Jonas Nils Becker<sup>1,4</sup>\*\* and Shannon Singer Nicley<sup>2,4,5</sup>\*\*

<sup>1</sup>Department of Physics and Astronomy, Michigan State University, East Lansing, MI, United States, <sup>2</sup>Department of Electrical and Computer Engineering, Michigan State University, East Lansing, MI, United States, <sup>3</sup>Toyota Research Institute of North America, Ann Arbor, MI, United States, <sup>4</sup>Coatings and Diamond Technologies Division, Center Midwest (CMW), Fraunhofer USA Inc, East Lansing, MI, United States, <sup>5</sup>Department of Chemical Engineering and Materials Science, Michigan State University, East Lansing, MI, United States

Introduction: Nitrogen-vacancy (NV) centers in diamond are widely recognized as highly promising solid-state quantum sensors due to their long room temperature coherence times and atomic-scale size, which enable exceptional sensitivity and nanoscale spatial resolution under ambient conditions. Ultrafast laser writing has demonstrated the deterministic spatial control of individual NV- centers, however, the resulting random orientation of the defect axis limits the magnetic field sensitivity and signal contrast.

**Methods:** We developed an all-optical approach for reorienting laser-written NV<sup>-</sup> centers to lie along a specific crystallographic axis using femtosecond laser annealing. The orientation is determined by polarization analysis, and the annealing and subsequent polarization analysis are repeated until the desired orientation is observed.

Results: Our method achieves deterministic alignment of NV<sup>-</sup> centers along the optical axis in (111)-oriented diamond substrates and allows selection between two observable orientation classes in (100)-oriented substrates. The reorientation preserves spatial ordering while producing uniform orientation across arrays of NV<sup>-</sup> centers.

Discussion: This approach enables scalable fabrication of orientation-controlled NV<sup>-</sup> arrays, and paves the way for scalable, high performance quantum devices based on orientation-controlled NV<sup>-</sup> centers.

femtosecond laser writing, nitrogen-vacancy center, NV reorientation, defect engineering, photonic quantum technologies, diamond, NV alignment

#### 1 Introduction

Among the various platforms for quantum technologies, negatively charged nitrogen vacancy (NV<sup>-</sup>) centers in diamond are particularly attractive due to their operation at room temperature, solid-state integration, and compatibility with advanced nanofabrication techniques. These features make them uniquely suited for scalable quantum technologies, including quantum information processing, sensing, and nanoscale imaging. The NV<sup>-</sup> center, a point defect consisting of a substitutional nitrogen atom adjacent to a vacant site in a diamond lattice, possesses electron spin states that can be

optically initialized, manipulated and read out, even at room temperature (Jelezko et al., 2004). These characteristics enable a range of applications, including magnetometry (Balasubramanian et al., 2008; Katsumi et al., 2025), electrometry (Dolde et al., 2011), and thermometry (Neumann et al., 2013). They are also highly versatile, and schemes have been reported allowing for their use as sensitive magnetometers in zero bias field (Zheng et al., 2019) and without the use of microwave excitation (Wickenbrock et al., 2016; Bürgler et al., 2023). Recent demonstrations on the transfer of the spin polarization to proximal nuclear spins to create a spin register have also shown incredible promise for the future of these centers, with spin coherence times exceeding several seconds (Bradley et al., 2019; van de Stolpe et al., 2024). A key advantage of using NV<sup>-</sup> centers lies in their nature as atomic-scale point defects in a solid-state host. Their minute size allows for nanometer scale precision in sensing, for example, allowing for the imaging of magnetic nanostructures and currents in microelectronic circuits.

Such applications, however, require deterministic placement of individual NV<sup>-</sup> centers with minimal damage to the surrounding lattice. This has been accomplished using ultrafast laser writing, which allows NV<sup>-</sup> centers to be fabricated with high spatial precision (Chen et al., 2017). The laser writing process consists of an initial seed pulse that produces vacancies in the lattice via multiphoton ionization, followed by a train of diffusion pulses, which cause vacancies to migrate until an NV<sup>-</sup> center is formed. This method has been used to fabricate NV<sup>-</sup> centers with an inplane positioning accuracy of 33 nm and a depth distribution with a half-width-at-half-maximum (HWHM) of 197 nm (Chen et al., 2019).

However, laser writing results in NV<sup>-</sup> centers oriented along any of the four possible axes, the [111],  $[1\overline{1}\overline{1}]$ ,  $[\overline{1}\overline{1}]$ , or  $[\overline{1}1\overline{1}]$  axes. Random orientation is undesirable for many magnetometry applications, as each NV center is sensitive only to the component of the magnetic field parallel to its orientation axis. This results in an orientation-dependent Zeeman splitting such that only a single orientation can be resonantly addressed at once. Other orientations then contribute to the background, decreasing the contrast of measurements. Preferential orientation of NVcenters along two axes has been demonstrated to increase the sensitivity of magnetometry with ensembles by a factor of 2 (Pham et al., 2012). CVD growth has been used to produce NVcenters with preferential orientation along two axes in diamonds with (110)-(Edmonds et al., 2012) and (100)-oriented surfaces (Pham et al., 2012), and along a single axis for (111)-(Lesik et al., 2014; Michl et al., 2014; Fukui et al., 2014) and (113)-oriented surfaces (Lesik et al., 2015). To date, however, no method has been demonstrated for the production of well localized *single* NV<sup>-</sup> centers with a specific orientation. The lack of post-fabrication orientation control has been an obstacle to scaling NV-based sensors, particularly in applications requiring uniform spin response such as vector magnetometry and high-contrast imaging of biological systems.

The NV<sup>-</sup> center emits fluorescence (PL) via a linear combination of two orthogonal dipole moments in the plane normal to the NV<sup>-</sup> center orientation axis. The dipoles are energetically degenerate, resulting in a nominally circular polarization pattern. However, they can contribute differently to

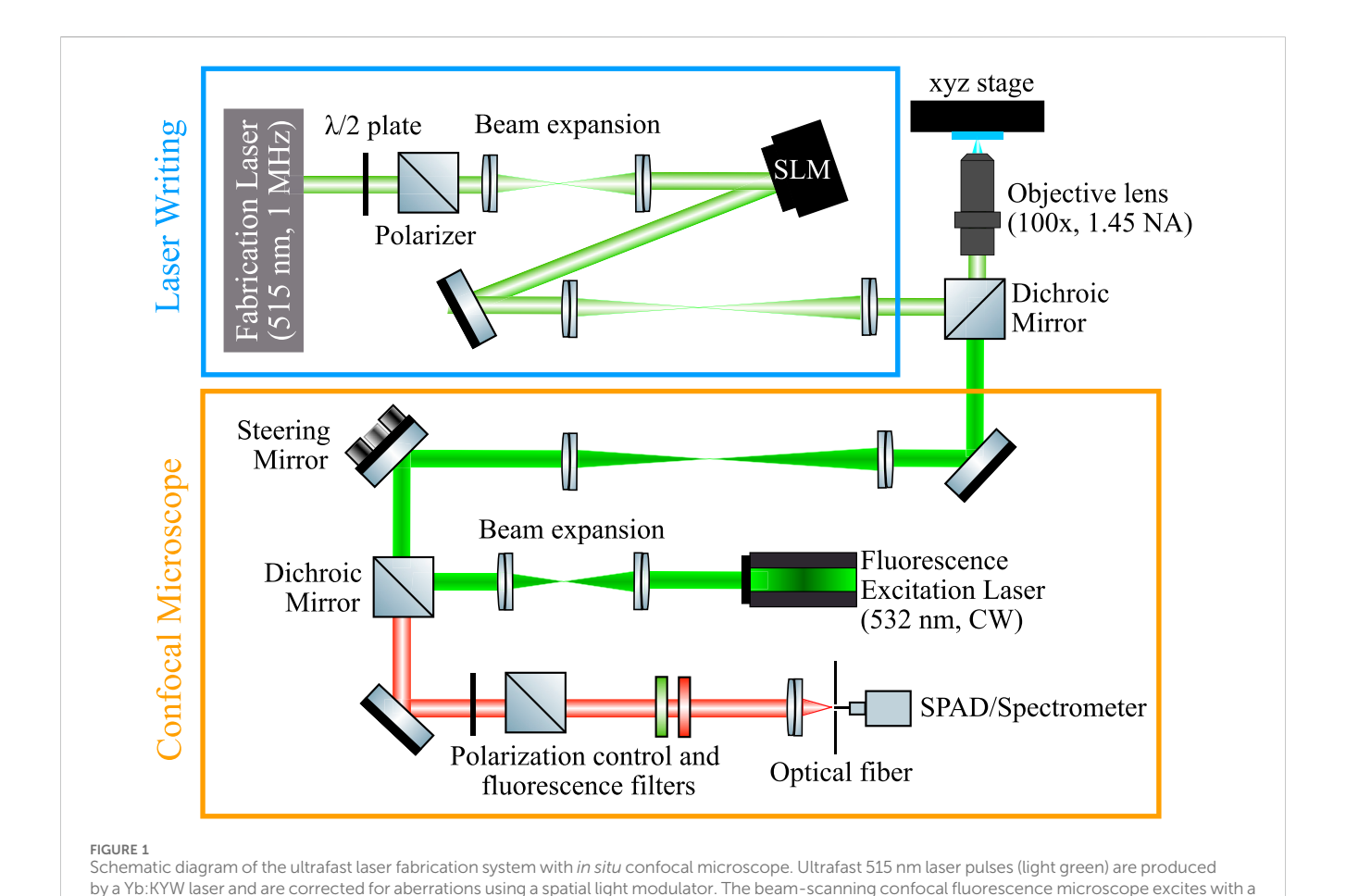
the overall PL signal when analyzed through a polarizer in the laboratory reference frame due to their respective orientations relative to the diamond surface. Hence, polarization patterns can be used to characterize the NV<sup>-</sup> orientation within the diamond lattice (Dolan et al., 2014). Due to the distinct dipole emission patterns in combination with diamond's high refractive index, orientation also affects the luminescence intensity, and the orientation can also be determined by observing this change in intensity (Peng et al., 2024).

Here, we combine several of these ideas and introduce a femtosecond laser annealing technique that allows for reorientation of individual laser written NV<sup>-</sup> centers. By selectively dissociating and reforming centers optically, all NV<sup>-</sup> orientations are produced stochastically. By combining this with *in situ* orientation detection via fluorescence polarization analysis, this process then enables the selection of a desired crystallographic orientation, allowing for fully deterministic spatial and orientational control of single NV<sup>-</sup> centers.

### 2 Methods

NV centers are fabricated using a home-built aberrationcorrected ultrafast laser writing system with an in situ confocal microscope, as shown in Figure 1. The system uses 270 fs pulses at 515 nm generated by a Yb:KYW laser (Light Conversion Pharos PH2). Pulse energy is controlled using a  $\lambda/2$  waveplate (Thorlabs WPHSM05-514) and a Glan-laser polarizer (Thorlabs GL5). The beam is then expanded to fill a spatial light modulator (SLM) (dualband Meadowlark HSP 1920-500-1200), which applies aberration corrections to compensate for the significant spherical aberration caused by diamond's high refractive index (Simmonds et al., 2011). The corrected beam is then focused into the diamond using a 1.45 numerical aperture (NA) oil immersion objective lens (Olympus MPlanApo N 100x). The sample is mounted on highprecision translation stages (Zaber LDM060C for x-y, LDM040C for z; accuracy 1 µm, repeatability < 80 nm) and widefield transmission imaging is performed using a CMOS camera (Thorlabs CS165MU/M).

The confocal fluorescence microscope shares the same objective lens as the laser writing system. Non-resonant excitation is provided by a 532 nm continuous-wave laser (Spectra Physics Millennia eV 15) which is scanned across the sample using galvanometric mirrors (Thorlabs QS7XY-AG) enabling spatially independent excitation relative to the fabrication focus. The emitted fluorescence is separated from both the excitation and fabrication wavelengths using a 550 nm longpass dichroic mirror (Thorlabs DMLP567), then coupled into an optical fiber for confocal optical sectioning. The collected fluorescence signal is directed either to a single-photon avalanche detector (SPAD) (Excelitas SPCM-AQRH-14), a spectrometer (Princeton Instruments SpectraPro HRS-750 with Blaze 400HR eXcelon camera), or a pair of SPADs arranged in a Hanbury Brown and Twiss (HBT) interferometer configuration for photon autocorrelation measurements. Both the laser writing system and confocal microscope are controlled via custom software written for a Field Programmable Gate Array (FPGA) (NI USB-7845R) with a user interface developed in LabVIEW and Python.



532 nm CW laser (dark green) and collects fluorescence (red) from the NV<sup>-</sup> center onto a single photon detector. Both the writing system and the microscope share a common objective lens onto the sample, which is illuminated in transmission for widefield microscopy onto a CMOS camera.

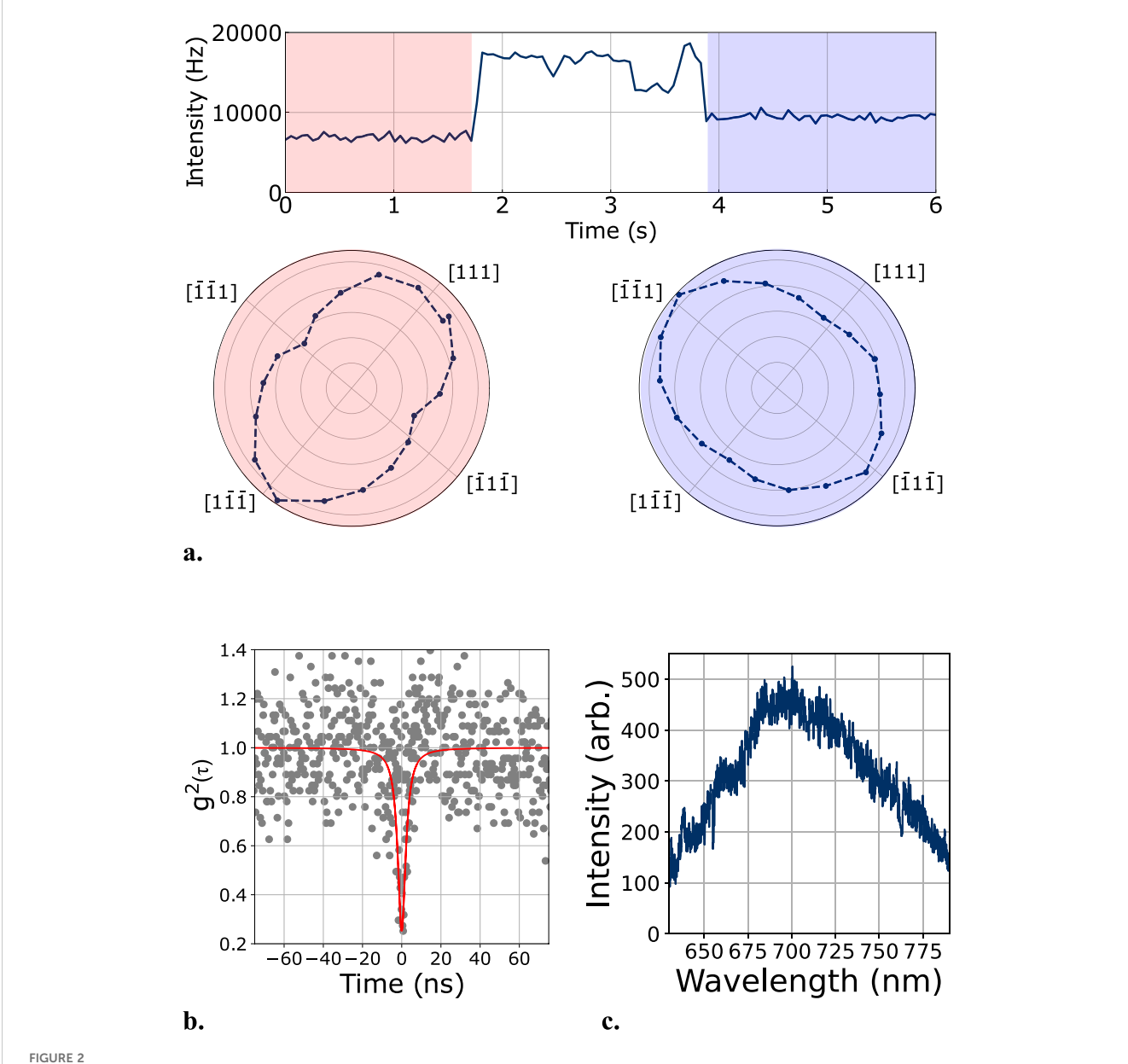
NV<sup>-</sup> center fabrication was performed on diamond substrates from two sources: a crystal with a (111)-oriented surface purchased from Flawless Technical Diamonds (FTD), in which a 3 × 3 array of NV<sup>-</sup> centers was created, and a (100)-oriented diamond substrate provided by Great Lakes Crystal Technologies (GLCT), where a single reoriented NV- center was produced. The (111)-oriented diamond was HPHT grown and contained 10 ppb substitutional nitrogen. The surface was polished to a surface roughness of 5 nm with a miscut angle of 3°. The (100)-oriented diamond was CVD grown and contained 80 ppb substitutional nitrogen. The surface was polished to a surface roughness of 1 nm with a miscut angle of 4°. The substitutional nitrogen grown into the substrates is the source of the nitrogen that was converted to NV centers during the laser writing process, and no additional nitrogen was implanted into the as-grown substrates. In both samples, NV- centers were fabricated using an initial 270 fs seed pulse (1.47 nJ at 515 nm) to generate vacancies and interstitial carbon atoms via multiphoton ionization. This was followed by a 200 kHz train of 1.19 nJ diffusion pulses which mobilized vacancies until one combined with a substitutional nitrogen atom to form an NV-Fluorescence intensity was monitored during this process, and the pulse train was terminated upon detection of an NV<sup>-</sup> signal.

Polarization analysis of the NV $^-$  fluorescence for orientation determination was achieved using a  $\lambda/2$  waveplate (Thorlabs

WPHSM05-694) in front of a polarizing beam splitter (Thorlabs PBS252). By rotating the half-wave plate, the full polarization profile of the emitted light was measured. The different projections of the NV center's emission dipoles onto the optical pupil enabled the identification of orientation based on the polarization pattern. All four orientations can be differentiated in this manner for diamond with a (111)-oriented surface, whereas only two sets of orientations are distinguishable for diamond with a (100)-oriented surface. If the measured orientation did not match the desired orientation, an additional annealing pulse train was applied, causing reorientation of the NV<sup>-</sup> center. Polarization measurements were repeated to identify the new orientation. This process was repeated until the desired orientation was observed. The fabricated NV- centers were then characterized using photoluminescence excitation spectroscopy and photon autocorrelation measurements. Occasionally, when reorientation did not readily occur after applying diffusion pulses for several minutes, a second seed pulse was applied to help the process.

#### 3 Results and discussion

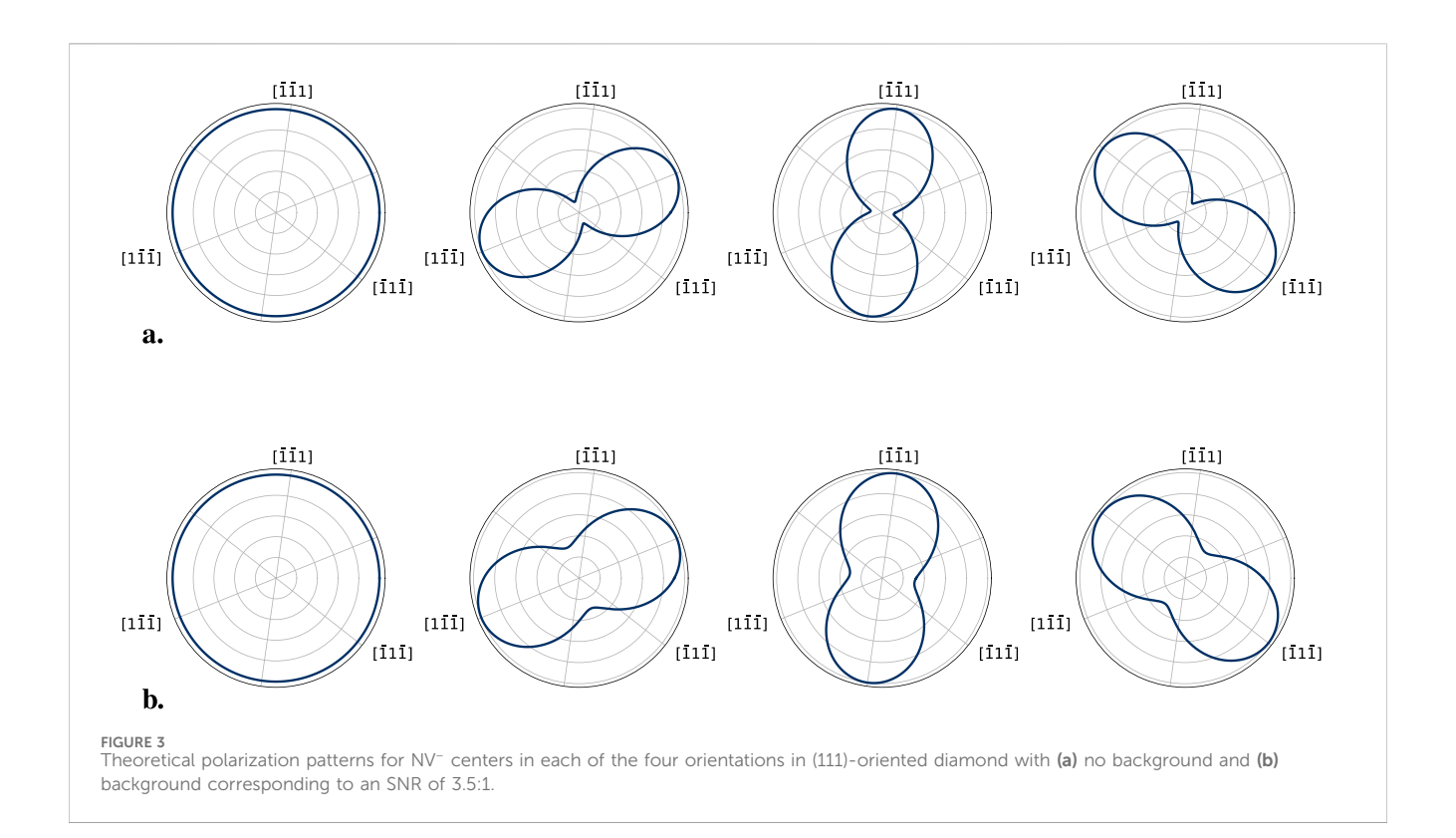
First, a single NV<sup>-</sup> center was fabricated and reoriented in a (100)-oriented diamond substrate. The initial polarization signature



(a) Fluorescence trace of an NV $^-$  center during reorientation in (100)-orientated diamond. Initially an NV $^-$  center is created along either of the polarization degenerate [111] or [1 $\overline{1}$ ] directions, as shown by the red-shaded polarization map. The diffusion pulse train is active between 1.8 and 3.9 s on the fluorescence trace. After some fluctuation in the measured fluorescence during diffusion, the NV $^-$  orientation is probed, resulting in the blue-shaded polarization map. This demonstrates an NV $^-$  orientation change between the polarization degenerate orientations of [ $\overline{1}$   $\overline{1}$ 1]/[ $\overline{1}$ 1 $\overline{1}$ ]  $\rightarrow$  [111]/[ $\overline{1}$ 1 $\overline{1}$ ]. The fluorescence is confirmed to be from a single NV $^-$  by (b) second-order photon autocorrelation measurement and (c) room temperature fluorescence spectrum.

of the center is shown in red in Figure 2a. Prior to reorientation, the half-waveplate in the fluorescence collection path was rotated to minimize the detected fluorescence signal. This provides polarization-dependent fluorescence contrast between the two distinguishable orientation classes observable in (100)-oriented diamond, allowing for quick reorientation detection. Figure 2a shows the time-resolved fluorescence signal during the reorientation process. The diffusion pulse train was activated at 1.8 s. A transient dip in fluorescence was observed just after the 3 s mark, followed by recovery to a higher fluorescence level. The diffusion pulse train was then terminated. The increased

fluorescence observed after the reorientation process is consistent with the change in polarization and thus increased transmission through the polarization analyzer. The new orientation was confirmed by a full measurement of the polarization pattern as shown shaded in blue in Figure 2a. Single photon emission was verified by photon autocorrelation with an excitation laser power of 1.2 mW, yielding a background-corrected  $g^{(2)}(0) = 0.25$ , as shown in Figure 2b. In (100)-oriented diamond, NV<sup>-</sup> centers fall into two optically distinguishable orientation classes. This partial control over orientation enables the creation of NV<sup>-</sup> arrays with only two orientations, potentially doubling the sensitivity in

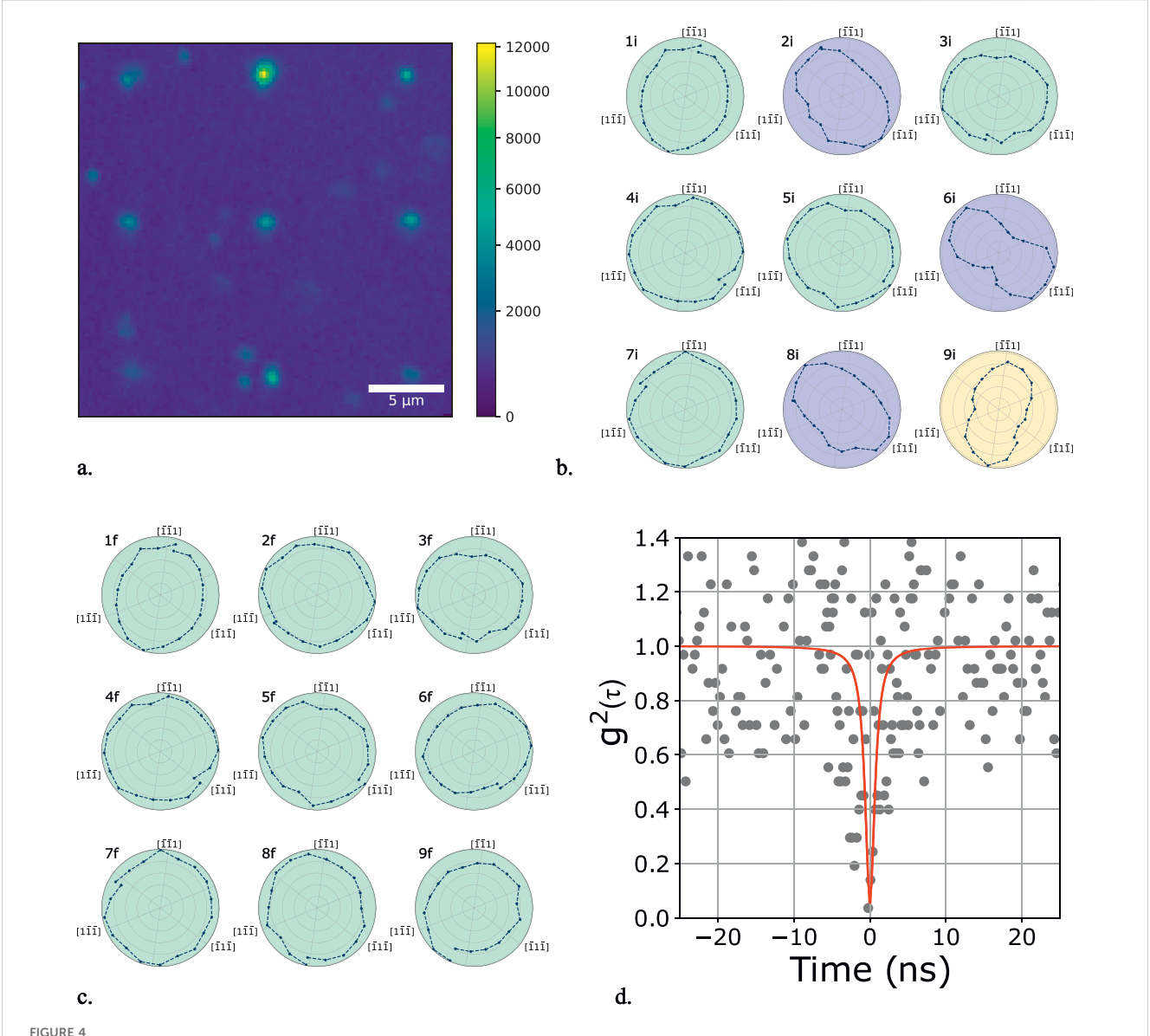


magnetometry applications (Pham et al., 2012). This degeneracy could be lifted by interrogation with radially polarized excitation (Dolan et al., 2014) or through optically detected magnetic resonance (ODMR).

To fully exploit the ability to distinguish all four NVorientations, we extended our method to a (111)-oriented diamond substrate. Theoretical polarization patterns, shown in Figure 3, were calculated by rotating the NV- center's two orthogonal emission dipoles from the NV<sup>-</sup> coordinate system to the laboratory reference frame, projecting onto the [111] plane, then using the Jones calculus to simulate the fluorescence transmitted through the half-wave plate and polarizing beam splitter for each orientation, following the approach in (Hepp et al., 2014). Figure 3a illustrates idealized patterns with no background fluorescence, while Figure 3b shows patterns corresponding to a signal-to-noise ratio (SNR) of 3.5:1, matching the approximate average observed SNR to facilitate comparison with experimental results. An array of nine NVcenters was fabricated with 10 µm pitch at a depth of 20 µm, as shown in Figure 4a. While shallow NV- centers are typically optimal for sensing applications, the array was fabricated at 20 µm in order to minimize boiling and lensing effects in the immersion oil, which can disrupt NV fabrication. Potential methods to overcome this limitation include fabricating near the far surface of the diamond, writing using a solid-immersion lens (Yurgens et al., 2021), or polishing after fabrication to remove excess surface material. Qualitative polarization analysis (Figure 4b) revealed that five of the nine fabricated NVcenters were initially oriented along the (111) crystallographic direction (i.e., parallel to the optical axis), while the remaining four NV<sup>-</sup> centers were distributed among two of the three other possible orientations. The fourth orientation of the centers was absent, due to the limited number of centers in the fabricated array (but has been observed in other fabrication runs). Initial orientations were confirmed by demonstrating that the root mean square (RMS) error between the measured polarization patterns and the theoretical patterns for each orientation shown in Figure 3b is minimized for the identified orientation, as shown in Table 1.

The reorientation process itself was identical to the (100) sample, with the exception that the polarization was not biased to minimize counts. Instead, a full polarization map was taken when fluctuations in the fluorescence level occurred. This was because the difference in fluorescence intensity using a single linear polarization analyzer between the four orientations does not provide a clear contrast in (111)-oriented diamond. Each NV- center was reoriented to the (111) direction parallel to the optical axis (vertical), which was confirmed by polarization measurements shown in Figure 4c. Successful reorientation was further confirmed through RMS error calculations, shown in Table 2. Single photon emission from one of the sites (site 3f) was verified by photon autocorrelation with an excitation laser power of 0.45 mW, yielding a background-corrected  $g^{(2)}(0) = 0.1$  as shown in Figure 4d. Note that the speed and simplicity of this process could in principle be improved further by splitting the fluorescence into multiple paths with separate polarization analyzers set to the individual orientation axes of (111)-oriented material. Comparison of the PL intensity in the individual arms could then provide quick feedback on the NV<sup>-</sup> orientation without the need to measure a full polarization pattern.

Such an  $NV^-$  array aligned along the optical axis has two distinct advantages over an unaligned array. Firstly, it allows for



(a) Confocal fluorescence image of laser written array of 9 NV<sup>-</sup> centers aligned parallel to the optical axis in (111)-oriented diamond. (b) Initial polarization maps of the NV<sup>-</sup> centers before reorientation, demonstrating random orientation. (c) Polarization maps for each NV<sup>-</sup> center in the array after reorientation to the optical axis, which identify all the NV<sup>-</sup> centers as being aligned along the optical axis in (111)-oriented diamond. (d) second-order photon autocorrelation measurement from NV<sup>-</sup> center 3f, confirming it to be a single center.

each member of the array to be coherently addressed simultaneously under the same magnetic field. This would in principle lead to a factor of four increase in sensitivity when compared to a randomly oriented array. Secondly, NV<sup>-</sup> centers aligned along the optical axis emit more light into a smaller NA of an objective lens and less light is lost during total internal reflection, ensuring both maximal light collection and reduction in non-symmetric aberrations accumulated at the diamond surface, improving sensitivity due to its enhanced photon collection. This improvement was estimated by calculating the light collection efficiencies from two NV<sup>-</sup> centers into a fixed NA. NV1 has its high-symmetry axis (z-axis) aligned parallel to the optical axis (perpendicular to the sample surface). NV2 is rotated by 109.5° with respect to

NV1. These two orientations reflect the two possible cases in a sample with (111) surface orientations. The main emission dipoles of the NV<sup>-</sup> center are two orthogonal dipoles in the xy-plane, perpendicular to the high-symmetry axis. Assuming far-field emission  $|d \times \vec{r}|^2$ , the emitted intensity was integrated over the solid angle for a given NA. Table 3 shows the collection efficiencies normalized by the total emitted power for NV1 and NV2 as well as their relative difference for a few common NAs. An array pitch of 10  $\mu$ m was chosen due to evidence in the literature that the diffusion process can influence an area of diamond much larger than the focal spot (Cheng et al., 2024). Further investigations of the diffusion process are needed to minimize potential unwanted effects on neighboring NV-centers, such as reorientation to an undesirable orientation,

TABLE 1 RMS error between the polar data for each array site shown in Figure 4b and the simulated polar plots with background shown in Figure 3b.

Array site	[111]	$[1\overline{1}\overline{1}]$	[1 11]	[111]
1i	0.195	0.310	0.246	0.346
2i	0.255	0.390	0.304	0.185
3i	0.204	0.263	0.354	0.290
4i	0.107	0.342	0.375	0.366
5i	0.137	0.348	0.370	0.294
6i	0.405	0.400	0.444	0.061
7i	0.109	0.345	0.345	0.367
8i	0.284	0.349	0.353	0.147
9i	0.378	0.322	0.121	0.378

The orientation of each  $\mathrm{NV}^-$  center is the orientation with the lowest RMS error, indicated in bold.

TABLE 2 RMS error between the polar data for each array site shown in Figure 4c and the simulated polar plots with background shown in Figure 3b.

Array site	[111]	$[1\overline{1}\overline{1}]$	[1 11]	[111]
1f	0.195	0.310	0.246	0.346
2f	0.120	0.333	0.357	0.331
3f	0.204	0.263	0.354	0.290
4f	0.107	0.342	0.375	0.366
5f	0.137	0.348	0.370	0.294
6f	0.196	0.263	0.338	0.331
7f	0.109	0.345	0.345	0.367
8f	0.138	0.366	0.306	0.331
9f	0.208	0.254	0.288	0.348

For each  $\mathrm{NV}^-$  center, the RMS error is lowest for the [111] direction, indicated in bold, confirming consistent orientation within the array.

and reduce emitter spacing. Since the magnetic sensitivity of NV<sup>-</sup> based devices scales with the number of NV<sup>-</sup> centers as  $1/\sqrt{N}$  it is unlikely that an oriented array of laser written single centers written in this manner will a higher magnetic sensitivity than that of a densely grown ensemble of randomly oriented centers. However, the ability to reorient defects would prove useful in applications that employ photonic devices or that utilize single

centers for high spatial resolution sensing (Balasubramanian et al., 2008; Maze et al., 2008; Casola et al., 2018).

Two potential, non-competing, mechanisms explain how reorientation occurs. Firstly, the initial NV- center is dissociated during annealing, allowing a vacancy to migrate and reform an NVcenter in a new orientation (Pinto et al., 2012). This occurrence is proposed within the literature as the dominant mechanism by which NV centers migrate in diamond under thermal annealing, however it is yet to be determined if ultrafast laser diffusion is able to exceed the energy barrier required to dissociate an NV center in this process. Although this mechanism seems promising considering the reduction in fluorescence during diffusion demonstrated in Figure 2a, there may be other mechanisms that can cause an NV center to stop fluorescing without dissociation. Hybridization between the NV- center's e-manifold and the  $\pi$ -bonds of a (100)-split carbon self-interstitial has been demonstrated and could reduce the fluorescence emission from the NV<sup>-</sup> center (Kirkpatrick et al., 2024). Therefore, it is possible that the reorientation process is substantially different from the thermal mechanism, with the initial NV<sup>-</sup> center continuing to exist initially but as a dark, modified defect-complex involving additional entities such as interstitials or vacancies, followed by a dissociation step of this intermediate defect, resulting in a reoriented NV<sup>-</sup> center. Further evidence for such a process is the occasional need to reseed after prolonged, unsuccessful reorientation attempts. This is likely due to a lack of species in the vicinity of the NV center that catalyze the reorientation process, most likely additional vacancies. It is in principle possible to reorient any observed NV- center. However, it is possible to inadvertently fabricate additional NV- centers depending on the properties of the sample (e.g., substitutional nitrogen content) or to inadvertently produce graphite depending on the laser parameters used. These risks can be mitigated with careful sample selection and tuning of the laser parameters.

In conclusion, we have demonstrated a fully optical method for the deterministic orientation of single NV<sup>-</sup> centers with high spatial resolution in diamond using femtosecond laser annealing. Using this method, we demonstrated the feasibility of fabricating oriented arrays of NV<sup>-</sup> centers in diamonds in both (100)- and (111)-oriented diamond substrates. Being an all-optical process, ultrafast laser writing provides unique control of the defect formation process and defect properties. Such techniques provide invaluable flexibility in fabricating optimized spin-photonic systems. Future work in this field may extend these methods to other defects in diamond or other materials systems, potentially in combination with the preparation of suitable precursor materials. Moreover, further optimization is needed to make this process suitable for writing of shallow defects and direct writing into nanostructured diamond. Finally, a better understanding

TABLE 3 Comparison of collection efficiencies and their relative differences for NV<sup>-</sup> centers oriented parallel to the optical axis (NV1) and 109.5° from the optical axis (NV2).

NA	NV1 collection efficiency (%)	NV2 collection efficiency (%)	Relative difference (%)
0.2	0.26	0.15	44.3
0.6	2.4	1.4	43.0
0.9	5.3	3.1	41.2
1.3	11.2	7.0	37.2

of the microscopic processes underpinning defect creation and dynamics in femtosecond laser fabrication via the development of theoretical models in combination with ultrafast spectroscopy is needed for further optimizations.

# Data availability statement

The original contributions presented in the study are included in the article, further inquiries can be directed to the corresponding authors.

#### Author contributions

KK: Writing – original draft, Investigation, Visualization, Software. AK: Conceptualization, Writing – original draft, Investigation, Software, Visualization. YT: Resources, Project administration, Writing – review and editing, Conceptualization, Funding acquisition. JB: Resources, Conceptualization, Funding acquisition, Writing – review and editing, Supervision, Project administration. SN: Writing – review and editing, Project administration, Supervision, Funding acquisition, Resources, Conceptualization.

## **Funding**

The author(s) declare that financial support was received for the research and/or publication of this article. This work was supported through a collaborative research agreement funded through Toyota Motor Engineering & Manufacturing, North America, Inc. JB was supported by the Cowen Family Endowment. KK acknowledges support from a Lawrence W. Hantel Endowed Fellowship at MSU.

#### References

Balasubramanian, G., Chan, I. Y., Kolesov, R., Al-Hmoud, M., Tisler, J., Shin, C., et al. (2008). Nanoscale imaging magnetometry with diamond spins under ambient conditions. *Nature* 455, 648–651. doi:10.1038/nature07278

Bürgler, B., Sjolander, T. F., Brinza, O., Tallaire, A., Achard, J., and Maletinsky, P. (2023). All-optical nuclear quantum sensing using nitrogen-vacancy centers in diamond. *npj Quantum Inf.* 9, 56. doi:10.1038/s41534-023-00724-6

Bradley, C. E., Randall, J., Abobeih, M. H., Berrevoets, R. C., Degen, M. J., Bakker, M. A., et al. (2019). A ten-qubit solid-state spin register with quantum memory up to one minute. *Phys. Rev. X* 9, 031045. doi:10.1103/PhysRevX.9. 031045

Casola, F., van der Sar, T., and Yacoby, A. (2018). Probing condensed matter physics with magnetometry based on nitrogen-vacancy centres in diamond. *Nat. Rev. Mater.* 3, 17088. doi:10.1038/natrevmats.2017.88

Chen, Y.-C., Salter, P. S., Knauer, S., Weng, L., Frangeskou, A. C., Stephen, C. J., et al. (2017). Laser writing of coherent colour centres in diamond. *Nat. Photonics* 11, 77–80. doi:10.1038/nphoton.2016.234

Chen, Y.-C., Griffiths, B., Weng, L., Nicley, S. S., Ishmael, S. N., Lekhai, Y., et al. (2019). Laser writing of individual nitrogen-vacancy defects in diamond with near-unity yield. *Optica* 6, 662. doi:10.1364/OPTICA.6.000662

Cheng, X., Thurn, A., Chen, G., Jones, G. S., Coke, M., Adshead, M., et al. (2024). Laser activation of single group-iv colour centres in diamond. *Nat Commun.* 16, 5124. doi:10.1038/s41467-025-60373-5

Dolan, P. R., Li, X., Storteboom, J., and Gu, M. (2014). Complete determination of the orientation of NV centers with radially polarized beams. *Opt. Express* 22, 4379–4387. doi:10.1364/OE.22.004379

# Acknowledgments

We thank Great Lakes Crystal Technologies (GLCT) for providing a suitable diamond sample for this work and Paul Quayle for helpful comments.

#### Conflict of interest

Author YT was employed by Toyota Motor North America. The remaining authors declare that the research was conducted in the absence of any commercial or financial relationships that could be construed as a potential conflict of interest.

### Generative AI statement

The author(s) declare that no Generative AI was used in the creation of this manuscript.

Any alternative text (alt text) provided alongside figures in this article has been generated by Frontiers with the support of artificial intelligence and reasonable efforts have been made to ensure accuracy, including review by the authors wherever possible. If you identify any issues, please contact us.

## Publisher's note

All claims expressed in this article are solely those of the authors and do not necessarily represent those of their affiliated organizations, or those of the publisher, the editors and the reviewers. Any product that may be evaluated in this article, or claim that may be made by its manufacturer, is not guaranteed or endorsed by the publisher.

Dolde, F., Fedder, H., Doherty, M. W., Nöbauer, T., Rempp, F., Balasubramanian, G., et al. (2011). Electric-field sensing using single diamond spins. *Nat. Phys.* 7, 459–463. doi:10.1038/nphys1969

Edmonds, A. M., Dâhaenens-Johansson, U. F. S., Cruddace, R. J., Newton, M. E., Fu, K.-M. C., Santori, C., et al. (2012). Production of oriented nitrogen-vacancy color centers in synthetic diamond. *Phys. Rev. B* 86, 035201. doi:10.1103/PhysRevB.86.035201

Fukui, T., Doi, Y., Miyazaki, T., Miyamoto, Y., Kato, H., Matsumoto, T., et al. (2014). Perfect selective alignment of nitrogen-vacancy centers in diamond. *Appl. Phys. Express* 7, 055201. doi:10.7567/APEX.7.055201

Hepp, C., Müller, T., Waselowski, V., Becker, J. N., Pingault, B., Sternschulte, H., et al. (2014). Electronic structure of the silicon vacancy color center in diamond. *Phys. Rev. Lett.* 112, 036405. doi:10.1103/PhysRevLett.112.036405

Jelezko, F., Gaebel, T., Popa, I., Gruber, A., and Wrachtrup, J. (2004). Observation of coherent oscillations in a single electron spin. *Phys. Rev. Lett.* 92, 076401. doi:10.1103/PhysRevLett.92.076401

Katsumi, R., Takada, K., Kawai, K., Sato, D., and Yatsui, T. (2025). High-sensitivity nanoscale quantum sensors based on a diamond micro-resonator. *Commun. Mater.* 6, 49. doi:10.1038/s43246-025-00770-x

Kirkpatrick, A. R., Chen, G., Witkowska, H., Brixey, J., Green, B. L., Booth, M. J., et al. (2024). *Ab initio* study of defect interactions between the negatively charged nitrogen vacancy centre and the carbon self-interstitial in diamond. *Philosophical Trans. R. Soc. A Math. Phys. Eng. Sci.* 382, 20230174. doi:10.1098/rsta.2023.0174

Lesik, M., Tetienne, J.-P., Tallaire, A., Achard, J., Mille, V., Gicquel, A., et al. (2014). Perfect preferential orientation of nitrogen-vacancy defects in a synthetic diamond sample. *Appl. Phys. Lett.* 104, 113107. doi:10.1063/1.4869103

Lesik, M., Plays, T., Tallaire, A., Achard, J., Brinza, O., William, L., et al. (2015). Preferential orientation of NV defects in CVD diamond films grown on (113)-oriented substrates. *Diam. Relat. Mater.* 56, 47–53. doi:10.1016/j.diamond.2015.05.003

Maze, J. R., Stanwix, P. L., Hodges, J. S., Hong, S., Taylor, J. M., Cappellaro, P., et al. (2008). Nanoscale magnetic sensing with an individual electronic spin in diamond. *Nature* 455, 644–647. doi:10.1038/nature07279

Michl, J., Teraji, T., Zaiser, S., Jakobi, I., Waldherr, G., Dolde, F., et al. (2014). Perfect alignment and preferential orientation of nitrogen-vacancy centers during chemical vapor deposition diamond growth on (111) surfaces. *Appl. Phys. Lett.* 104, 102407. doi:10.1063/1.4868128

Neumann, P., Jakobi, I., Dolde, F., Burk, C., Reuter, R., Waldherr, G., et al. (2013). High-precision nanoscale temperature sensing using single defects in diamond. *Nano Lett.* 13, 2738–2742. doi:10.1021/nl401216y

Peng, D. Y. M., Worboys, J. G., Sun, Q., Li, S., Capelli, M., Onoda, S., et al. (2024). Alloptical determination of one or two emitters using polarization-enhanced photon correlations of nitrogen-vacancy centers in diamond. *Phys. Rev. A* 109, 023723. doi:10.1103/PhysRevA.109.023723

Pham, L. M., Bar-Gill, N., Le Sage, D., Belthangady, C., Stacey, A., Markham, M., et al. (2012). Enhanced metrology using preferential orientation of nitrogen-vacancy centers in diamond. *Phys. Rev. B* 86, 121202. doi:10.1103/PhysRevB.86.121202

Pinto, H., Jones, R., Palmer, D. W., Goss, J. P., Briddon, P. R., and  $\tilde{A}$ -berg, S. (2012). On the diffusion of nv defects in diamond. *Phys. status solidi* (a) 209, 1765–1768. doi:10. 1002/pssa.201200050

Simmonds, R. D., Salter, P. S., Jesacher, A., and Booth, M. J. (2011). Three dimensional laser microfabrication in diamond using a dual adaptive optics system. *Opt. Express* 19, 24122–24128. doi:10.1364/OE.19.024122

van de Stolpe, G. L., Kwiatkowski, D. P., Bradley, C. E., Randall, J., Abobeih, M. H., Breitweiser, S. A., et al. (2024). Mapping a 50-spin-qubit network through correlated sensing. *Nat. Commun.* 15, 2006. doi:10.1038/s41467-024-46075-4

Wickenbrock, A., Zheng, H., Bougas, L., Leefer, N., Afach, S., Jarmola, A., et al. (2016). Microwave-free magnetometry with nitrogen-vacancy centers in diamond. *Appl. Phys. Lett.* 109, 053505. doi:10.1063/1.4960171

Yurgens, V., Zuber, J. A., Flågan, S., De LucaBrendan, M., Shields, B. J., Zardo, I., et al. (2021). Low-charge-noise nitrogen-vacancy centers in diamond created using laser writing with a solid-immersion lens. *ACS Photonics* 8, 1726–1734. doi:10.1021/acsphotonics.1c00274

Zheng, H., Xu, J., Iwata, G. Z., Lenz, T., Michl, J., Yavkin, B., et al. (2019). Zero-field magnetometry based on nitrogen-vacancy ensembles in diamond. *Phys. Rev. Appl.* 11, 064068. doi:10.1103/PhysRevApplied.11.064068